# Toward a velocity-resolved microvascular blood flow measure by decomposition of the laser Doppler spectrum

**Marcus Larsson**
**Tomas Strömberg**
Linköpings Universitet
Department of Biomedical Engineering
University Hospital
S-581 85 Linköping
Sweden
E-mail: marla@imt.liu.se

**Abstract.** Tissue microcirculation, as measured by laser Doppler flowmetry (LDF), comprises capillary, arterial, and venous blood flow. With the classical LDF approach, it has been impossible to differentiate between different vascular compartments. We suggest an alternative LDF algorithm that estimates at least three concentration measures of flowing red blood cells (RBCs), each associated with a predefined, physiologically relevant, absolute velocity in millimeters per second. As the RBC flow velocity depends on the dimension of the blood vessel, this approach might enable a microcirculatory flow differentiation. The LDF concentration estimates are derived by fitting predefined Monte Carlo simulated, single-velocity spectra to a measured, multiple-velocity LDF spectrum. Validation measurements, using both single- and double-tube flow phantoms perfused with a microsphere solution, show that it is possible to estimate velocity and concentration changes, and to differentiate between flows with different velocities. Our theory is also applied to RBC flow measurements. A Gegenbauer kernel phase function ($\alpha_{gk}=1.05$; $g_{gk}=0.93$), with an anisotropy factor of 0.987 at 786 nm, is found suitable for modeling Doppler scattering by RBCs diluted in physiological saline. The method is developed for low concentrations of RBCs, but can in theory be extended to cover multiple Doppler scattering. © *2006 Society of Photo-Optical Instrumentation Engineers.* [DOI: 10.1117/1.2166378]

## 1 Introduction

When photons propagate through a turbid medium they interact with both static and moving scatterers. Interaction with a moving scatterer, such as a red blood cell (RBC), causes a frequency shift according to the Doppler principle. For a given RBC velocity, the Doppler shift depends on the statistical variations in the scattering angle. Using coherent light, the backscattered photons will form a time-varying speckle pattern that generates a photodetector current that beats with the Doppler frequency.[1] The microcirculatory perfusion, defined as the product of the mean velocity and concentration of moving RBCs, can in theory be assessed from the integrated frequency-weighted power spectrum of the photocurrent, i.e., the first moment of the laser Doppler spectrum.[2–5] In traditional laser Doppler flowmetry (LDF), the perfusion is measured in relative units. Therefore, no information on the absolute RBC velocity or velocity distribution is obtained.

Due to the complex relationship between the RBC velocity and the scattering angle, Dörschel and Müller[6] developed a method for correcting the laser Doppler spectrum to obtain a more one-to-one relationship between the Doppler spectrum and the corresponding velocity. They assumed an isotropically distributed angle between the velocity and the scattering vector, and a constant scattering angle; the latter assumption being an oversimplification. Furthermore, they integrated the Doppler spectrum over selected frequency intervals (higher frequencies giving an emphasis on higher RBC velocities) to achieve a velocity-resolved tissue perfusion measure. Others[7–9] have suggested LDF algorithms that estimate the average RBC velocity by comparing measured and simulated Doppler spectra. These algorithms are only valid/validated for large source detector separations ($>15$ mm), and thus, they are not suitable for implementation in standard LDF systems, where small source detector separations ($<2$ mm) are used. In addition, these algorithms are capable of estimating only the average RBC velocity and not the RBC velocity distribution.

The method presented in this paper is based on the single Doppler scattering event but with fewer simplifications than the Dörschel and Müller approach. We assume an isotropic distribution of the Doppler-scattering vectors compared to the direction of the moving scatterer, and a negligible probability

Address all correspondence to Marcus Larsson. Dept. of Biomedical Engineering, Linköpings Universitet, University Hospital, S-581 85 Linköping, Sweden. Tel: 46 13 222474. Fax: 46 13 101902. E-mail: marla@imt.liu.se
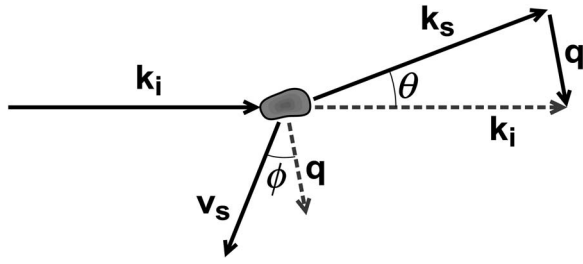
**Fig. 1** Doppler scattering by a single scatterer moving with the velocity $v_s$; $\theta$ denotes the scattering angle, $\phi$ is the angle between the scattering vector $\boldsymbol{q}$ and the direction of the moving scatterer.

for multiple Doppler-scattering events. The theory is developed and tested for moving scatterers being either microspheres of a known size or RBCs. As for the scattering angle distribution, the analytical Mie theory is used for the microspheres, and the RBC scattering data are fitted to a Gegenbauer kernel phase function. The theory relates the power spectrum of the detected photocurrent, i.e., the Doppler spectrum, to the distribution of Doppler frequencies, which can be simulated using the Monte Carlo technique. A set of base functions, consisting of simulated Doppler spectra arising from known velocities (in absolute units; millimeters per second) are fitted to a measured Doppler spectrum. The traditional LDF perfusion measure can then be replaced by the relative magnitude of the base spectra, i.e., a velocity-resolved perfusion measure is achieved. The maximum number of base functions is limited to avoid overfitting.

The aim of the study reported here was to propose a method for characterizing the microvascular blood flow in a number of velocity components, rather than a single mean value, as obtained in traditional LDF. The method assesses the relative number of scatterers moving with physiologically relevant, absolute velocities (in millimeters per second).

## 2 Material and Methods

### 2.1 LDF Theory

When coherent laser light illuminates a turbid medium, a fraction of the injected light will be diffusely backscattered. If a detector is placed above the medium, an interference pattern, or speckle pattern, will be formed on the detector surface. By introducing moving scatterers in the medium, Doppler shifts will occur, and a portion of the backscattered photons will be shifted slightly in frequency. The size of an individual Doppler shift is given by[10]

$$\omega_d = \frac{4\pi}{\lambda_t} v \sin(\theta/2) \cos(\phi), \qquad (1)$$

where $\lambda_t$ is the wavelength in the medium, $v$ is the velocity of the moving scatterer, $\theta$ is the scattering angle, and $\phi$ is the angle between the scattering vector ($\boldsymbol{q}$) and the direction of the moving scatterer (Fig. 1). In a turbid medium, $v$, $\theta$, and $\phi$ are described by physiological and statistical distributions. Consequently, backscattered light will contain photons with diverse frequency shifts, resulting in a total $E$ field containing a distribution of frequencies rather than a single Doppler frequency.

The frequency shifts, produced by the moving scatterers, will cause the speckle pattern to fluctuate, generating a time-varying detector current with a frequency content that resembles the Doppler histogram of the detected $E$ field. It has previously been shown[1,11] that the power spectrum $P(\omega)$ of the detected photocurrent, also referred to as the Doppler spectrum, is linked to the distribution of Doppler frequencies, i.e., the Doppler histogram $H(\omega)$, by

$$P(\omega) = \boldsymbol{q}_{ac} H(\omega) \star H(\omega)^*, \qquad (2)$$

where $\star$ denotes cross-correlation, and $\boldsymbol{q}_{ac}$ is an instrumental constant. The Doppler histogram (optical spectrum), consisting of a nonshifted static part $[H_0 = H(\omega_0)]$ and a shifted part $[H_d = H(\omega \neq \omega_0)]$, can be expressed as

$$H(\omega) = H(\omega)^* = H_0 \delta(\omega - \omega_0) + H_d(\omega), \qquad (3)$$

where $\delta$ is the dirac function, and $\omega_0$ is the frequency of the injected laser light. If the degree of Doppler-shifted photons is low, i.e., $H_0 \gg \Sigma_\omega H_d(\omega)$, $P(\omega)$ can be approximated by

$$P(\omega) = \boldsymbol{q}_{ac} [H_0^2 \delta(\omega) + 2H_0 H_d(\omega - \omega_0) + H_d(\omega) \star H_d(\omega)]$$
$$\approx \boldsymbol{q}_{ac} [dc^2 \delta(\omega) + 2dc H_d(\omega - \omega_0)], \qquad (4)$$

where $dc = \Sigma_\omega H(\omega)$ is the theoretical total light intensity. In the classic LDF measurement setup, the stationary part of Eq. (4) is removed by differentiation and highpass filters, i.e., $dc^2 \delta(\omega) = 0$. Further, the amplitude of the Doppler histogram scales linear against the total light intensity that is injected into the sample. By normalizing the Doppler histogram with the total light intensity, variations due to light intensity perturbations are removed.

In this paper, only cases with a low degree of Doppler-shifted photons were considered. Hence, the approximation

$$P_n(\omega) = \frac{P(\omega)}{dc_m^2} \approx \frac{2\boldsymbol{q}_{ac}}{\boldsymbol{q}_{dc}^2} \frac{H_d(\omega')}{dc} = \frac{\boldsymbol{q}_{ac}}{\boldsymbol{q}_{dc}^2} H_{nd}(\omega'), \qquad (5)$$

can be used for studying the true Doppler frequency distribution, where $dc_m = \boldsymbol{q}_{dc} dc$ is the measured total light intensity and $\boldsymbol{q}_{dc}$ an instrumental constant. The intensity-normalized Doppler spectrum and histogram are denoted as $P_n$ and $H_{nd}$, respectively.

According to Eq. (1) there is a direct link between the width of the Doppler histogram and the velocity of the moving scatterers. Hence, it is logical to assume that velocity information can be extracted from an LDF measurement by studying the laser Doppler spectrum.

### 2.2 Decomposition of the Doppler Spectrum

Phantoms or tissue that contain moving scatterers with more than one velocity will result in Doppler histograms that consist of superimposed single-velocity histograms. If the concentration of moving scatterers is low, i.e., a negligible degree of multiple Doppler shifts, it is logical to assume that

$$H_{tot}(\omega') = \sum_i c_{v_i} H_{v_i}(\omega'), \qquad (6)$$

where $H_{tot}$ is the multiple-velocity Doppler histogram, and $c_{v_i}$ is the concentration of scatterers that move with a velocity of

$v_i$. The normalized, single-velocity Doppler histogram produced by the velocity $v_i$ is denoted $H_{v_i}$. The velocity-dependent concentration term $c_{v_i}$ is also referred to as the velocity component or VC.

If $H_{v_i}$ is known for a few velocities, it is possible to derive $c_{v_i}$ by fitting the expression in Eq. (6) to a measured $dc_m^2$-normalized Doppler spectrum ($P_n$). Using least-squares fitting to derive $c_{v_i}$ results in large relative errors for the higher frequencies where the amplitude of LDF histograms is low. Consequently, a poor estimation of the high-velocity components is achieved. Instead, to achieve a good agreement between the model and measured data for all frequencies of interest, the single-velocity histogram must be normalized with the measured Doppler spectrum before fitting, i.e., solving

$$\min_{c_{v_i}} \left\langle \left| \sum_i c_{v_i} \frac{H_{v_i}(\omega')}{P_n(\omega)} - 1 \right|^2 \right\rangle_\omega, \qquad (7)$$

where $\langle\rangle_\omega$ denotes the average over all frequencies. In this way the relative error, and not the absolute error, is minimized, and a good $c_{v_i}$ estimation is achieved for all included velocities.

Due to system noise and filters, a frequency range within which the fitting is conducted must be set. In this paper, the lower frequency limit was set to 50 Hz to remove the effect of the highpass filter of the LDF system. The upper limit was chosen adaptively, based on the amplitude of the noise-reduced Doppler spectrum. This was necessary to avoid the high-frequency area where the amplitude of the Doppler spectrum drops below the noise-induced variance, a level that is constant over all frequencies. The choice of upper limit depends on both the number of spectra that was averaged and the flow velocity and concentration.

The velocities $v_i$ that are included in the model must cover the velocity range that is expected from the measurement. Adjacent velocities are difficult or impossible to separate due to the resemblance of their histograms. In this paper, the included velocities were chosen either on the basis of the true flow velocities in the flow model, for model verification, or as the three fixed velocities 0.5, 2.0, and 8.0 mm/s. The three fixed velocities were selected with a constant relative increase in their velocity, to avoid that the included histograms become nonunique.

## 2.3 Simulation of the Doppler Histogram

The size of a Doppler shift, and consequently the Doppler histogram itself, as indicated in Eq. (1), is affected by numerous factors:

1. phase function of moving scatterers
2. velocity distribution of moving scatterers
3. flow direction versus scattering vector ($\boldsymbol{q}$ vector)
4. refractive index of surrounding medium (affects $\lambda_t = \lambda/n_t$)
5. wavelength

The phase function of a particle depends on its size, shape, relative refractive index (compared to the surrounding medium), and the wavelength of the light. For blood, this affects the phase function of the RBC through the level of hematocrit, osmolarity, and hemolysis.[12] However, these parameters

can be considered as relatively constant, compared to the flow velocity. Thus, it is reasonable to categorize the phase function of moving RBCs as a constant distribution. In analogy, the refractive index of the surrounding medium (blood plasma) can also be considered as a constant. Further, the direction of the scattering vector ($\boldsymbol{q}$ vector), compared to the flow direction, can be considered as isotropic after a few reduced mean free pathlengths ($\mathrm{mfp}' \approx 1/\mu_s'$), while the wavelength is given by the LDF system. Given these assumptions, the only changing factor that has a major impact on the Doppler histogram is the velocity of the moving scatterers, a parameter that broadens the histogram according to Eq. (1).

### 2.3.1 Phase function of moving scatterers

For a microsphere of known material and size, it is possible to calculate a theoretical phase function using Mie theory. For an RBC, however, Mie theory is not easily applicable due to the complex shape of the RBC. The commonly used one-parameter Henyey-Greenstein phase function ($p_{hg}$) is also not suitable as a scattering model for the RBC due to its forward-peaked phase function properties. Instead, it has been suggested that the two-parameter Gegenbauer kernel phase function ($p_{gk}$) is a better model for describing the scattering properties[12,13] of the RBC. The Gegenbauer kernel phase function is given by

$$p_{gk}(\theta) = \frac{\alpha_{gk} g_{gk} (1 - g_{gk}^2)^{2\alpha_{gk}}}{\pi[(1 + g_{gk})^{2\alpha_{gk}} - (1 - g_{gk})^{2\alpha_{gk}}][1 + g_{gk}^2 - 2g_{gk}^2 \cos(\theta)]^{\alpha_{gk}+1}}, \qquad (8)$$

where $\alpha_{gk}$ and $g_{gk}$ are the two parameters affecting the phase function. Noticeable is that $p_{gk}$ equals $p_{hg}$ when $\alpha_{gk}$ is set to 0.5.

In this paper, two types of scattering particles were used: Polystyrene microspheres (motility standard PF 1001, Perimed AB, Sweden) and RBCs. The phase function of the Polystyrene microspheres was derived using Mie theory.[14] A radius of 0.155 $\mu$m and a real refractive index of 1.58 at 786 nm was used, as specified by the manufacturer. The microspheres were diluted in deionized water with a refractive index of 1.33 at 786 nm. Unpolarized light was assumed. The RBC phase function was derived empirically, assuming a Gegenbauer kernel distribution. The parameters $\alpha_{gk}$ and $g_{gk}$ were found by minimizing the relative error between the simulated Doppler histograms and the measured Doppler spectra.

### 2.3.2 Velocity distribution of moving scatterers

The proposed theory was evaluated in a single-tube and a double-tube flow model. The geometry of the tubes and the velocity range that was used resulted in a maximum Reynolds number[15] of 11. This suggests that the tube flows are laminar with a parabolic flow profile, resulting in a uniform distribution between zero and two times the average flow velocity.[16] Hence, to study the difference between the tubes, and not the actual velocity distribution within the tubes, the single-velocity Doppler histogram $H_{v_i}$ in Eqs. (6) and (7) needs to be modified to cover a parabolic flow profile.

### 2.3.3 Flow direction versus scattering vector

When light propagates through a turbid medium, it loses its preferential direction after a few $\mathrm{mfp}'$. It becomes isotropic.

Thus, the direction of the scattering vector, compared to the flow direction, will also be isotropic. For biological tissue, where the blood vessels are not ordered in any specific direction, the isotropy assumption is valid for distances even shorter than a few mfp′. The isotropy assumption results[6] in a uniform distribution of $\cos(\phi)$ between −1 and 1.

### 2.3.4 Simulation of the Doppler histogram

LDF Doppler histograms were simulated using a random number approach that could be described as a single Doppler-scattering Monte Carlo model. The model assumes that multiple scattering in surrounding static material, prior to the simulated Doppler-scattering occasion, causes the light to become isotropic, i.e., the angular Doppler-dependency is lost. Based on Eq. (1), a total of $10^7$ Doppler shifts were simulated and used for calculating each Doppler histogram. The scattering angle $\theta$ was generated numerically through a look-up table for the cumulative phase function, combined with random numbers originating from a uniform distribution between 0 and 1. The term $\cos(\phi)$ was generated directly by using a random number generator with a uniform distribution between −1 and 1. The velocity term $v$ was simulated using a random number generator with a uniform distribution between 0 and $2\bar{v}$, simulating a parabolic flow profile. Histograms were calculated using a fixed frequency bin size equal to the bin size of the measured Doppler spectra, about 12.2 Hz.

### 2.4 Experimental Setup

The velocity component theory was evaluated by the use of two different flow phantoms: a single-tube phantom and a double-tube phantom. The single-tube phantom consisted of a transparent polythene microtube with an inner radius of 0.55 mm and an outer radius of 0.75 mm. The tube was placed in a piece of Delrin® with its center 3.0 mm below the surface. The double-tube phantom consisted of two transparent polythene microtubes with an inner radius of 0.45 mm and an outer radius of 0.75 mm. The tubes were placed in a piece of Delrin® with centers 2.5 mm below the surface parallel to each other and 4.0 mm apart (center-to-center distance).

### 2.4.1 RBC measurement setup

The measurements on the single-tube phantom encompassed a number of different flow velocities, ranging from about 0 to 10 mm/s, using RBCs as moving scatterers. The blood was heparinized, minimizing the risk of coagulation, and highly diluted (1:1000) in a physiological saline solution (0.9% NaCl), avoiding multiple Doppler shifts and osmolarity effects. Further, the diluted blood was carefully stirred prior to all measurements to minimize the RBC sedimentation risk. A syringe pump was used to achieve a constant flow velocity. The collected data were used to demonstrate that a good agreement between simulations and measurements could be achieved by using an optimized Gegenbauer kernel phase function.

### 2.4.2 Microsphere measurement setup

Measurements using blood as a fluid are always complicated due to the risk of hemolysis and RBC sedimentation, espe-

cially when dealing with measurement series that are conducted during several hours or days. Therefore, a solution consisting of deionized water and polystyrene microspheres was used in the more extensive and time-consuming double-tube experiments. The size of the microspheres ensured that no sedimentation would occur during the time frame of each measurement. In addition, the microspheres had a known geometry and refractive index, and could thus be calculated theoretically using Mie theory, i.e., the phase function was derived independently of the measurement results, in direct contrast to the RBC phase function.

Both the influence of flow velocity, ranging from about 0 to 10 mm/s, and microsphere concentration, using four different solutions, were evaluated in the double-tube phantom. The microsphere solutions were diluted using deionized water, resulting in a scattering coefficient $\mu_s$ of 0.12, 0.24, 0.36, and 0.48 mm$^{-1}$, as given by collimated transmission measurements. In addition, some measurements included nonscattering deionized water as a fluid to create a single-tube flow. In total, four experimental setups (referred to as setup 1, …, setup 4), with different combinations of microsphere concentration and velocities, were evaluated using the double-tube phantom:

1. Single flow setup with a $\mu_s$ of 0.24 mm$^{-1}$ and 16 velocities covering the range 0 to 10 mm/s (16 measurements).

2. Single flow setup using all four solutions in combination with the two velocities 0.91 and 1.51 mm/s in tube 1 (8 measurements).

3. Combined single- and double-tube flow setup using four different velocity configurations (tube 1 and tube 2): 0.91 and 2.90 mm/s; 0.91 and 4.60 mm/s; 1.51 and 4.83 mm/s; and 1.51 and 7.66 mm/s. Each velocity configuration was evaluated using a microsphere concentration of 0.24 mm$^{-1}$ in either or both of the tubes, yielding two single-tube flow measurements and one double-tube flow measurement for each velocity configuration (12 measurements).

4. Double-flow setup using a fixed $\mu_s$ of 0.12 mm$^{-1}$ in tube 1 and all four solutions, including deionized water, in tube 2. All five concentration combinations were evaluated using four different velocity configurations (tube 1 and tube 2): 0.91 and 2.90 mm/s; 0.91 and 4.60 mm/s; 1.51 and 4.83 mm/s; and 1.51 and 7.66 mm/s (20 measurements).

### 2.5 LDF System and Signal Processing

In this study, a modified Periflux 5000 LDF system (Perimed AB, Järfälla, Sweden) was used. The system consisted of a standard fiber optic probe (Probe 408, Perimed AB, Järfälla, Sweden), a diode laser at 768 nm, and detector electronics. The fiber optic probe contained one emitting and one receiving step-index fiber, both having a core diameter of 125 $\mu$m and a numerical aperture of 0.37. The emitting and receiving fibers were separated by 230 $\mu$m (center-to-center distance) at the face of the probe tip. The detector electronics comprised two photodetector circuits, coupled together both differentially[2] and additively, resulting in an $ac_m$ (time varying signal) and a $dc_m$ (total light intensity) signal. The $ac_m$ signal was amplified and bandpass filtered between 8 Hz and 20 kHz. The $dc_m$ signal was amplified and lowpass filtered with a cutoff frequency of 32 Hz. Both signals were sampled at 50 kHz using a 12-bit analog-to-digital converter
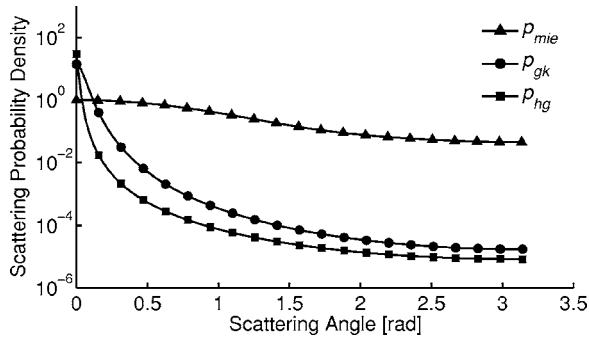
**Fig. 2** Phase functions of polystyrene microspheres ($p_{mie}$: Mie theory with $\langle\cos\theta\rangle=0.494$) and RBCs ($p_{gk}$: optimized Gegenbauer kernel distribution with $\alpha_{gk}=1.05$, $g_{gk}=0.93$ and $\langle\cos\theta\rangle=0.987$; $p_{hg}$: Anisotropy equivalent Henyey-Greenstein distribution with $\langle\cos\theta\rangle=0.987$).

(DAQpad-6070E, National Instruments Inc.) and stored on a computer for postprocessing.

The measured laser Doppler spectra were estimated from 4096 samples of data using Welch's averaged, modified periodogram method in Matlab 6.5 (Mathworks, Inc.). For each measurement, a total of 1220 spectra, gathered in 100 s, were averaged to minimize the noise-related variance in the Doppler spectra and to enhance the stationary portion that is generated by Doppler-shifted photons. This was necessary since our flow models were designed to avoid multiple Doppler shifts and to ensure that the light had lost its preference direction and become isotropic, features that result in an extremely low degree of Doppler-shifted photons. The total light intensity was calculated by averaging all $dc_m$ values that were gathered during each measurement. For comparison, the classical LDF concentration measure, denoted as CMBC, was calculated as

$$\text{CMBC} = \frac{1}{dc_m^2}\int P(\omega)\,d\omega. \qquad (9)$$

When an $E$ field is detected by a photodetector, a white noise is superimposed on the detector signal. The superimposed noise level depends not only on the choice of components, but also on the amplitude of the detected $E$ field: the power of the noise increases linearly with the total light intensity. The spectral noise characteristics of the system were derived through multiple LDF measurements at a static phantom at different equidistant dc levels. Noise-reduction of the recorded Doppler spectrum was carried out by subtracting a linear interpolation of the two noise-spectra whose dc levels were closest to the dc level of the LDF recording.

## 3 Results

The optimal Gegenbauer kernel phase functions, derived as an average over all RBC measurements (Sec. 2.4.1), was found at $\alpha_{gk}=1.05$ and $g_{gk}=0.93$, yielding an anisotropy factor of $\langle\cos\theta\rangle=0.987$. In Fig. 2, the optimized Gegenbauer kernel RBC phase function is shown along the anisotropy-equivalent Henyey-Greenstein phase function ($\langle\cos\theta\rangle=0.987$) and the microsphere Mie phase function ($\langle\cos\theta\rangle=0.494$).

A good agreement between simulated and measured single-tube flow Doppler spectra was found for both the poly-
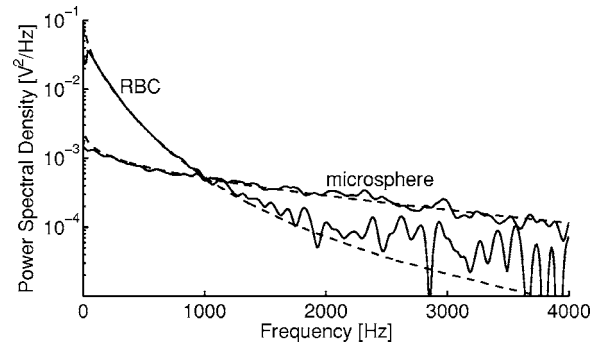


**Fig. 3** Measured (solid lines) and simulated (dashed lines) single-tube flow Doppler spectra for the polystyrene microsphere (setup 1) and RBC solutions. The simulated spectra were derived using a phase function based on Mie theory (microsphere) and a Gegenbauer kernel phase function (RBC), in combination with a parabolic flow profile with an average flow velocity equal to the observed flow velocity (polystyrene microsphere: 2.51 mm/s; RBC: 2.38 mm/s).

styrene microspheres (setup 1) and the RBCs, as demonstrated in Fig. 3. In a few exceptions, a small deviation in the lower frequencies (below 200 Hz) was found.

The velocity component estimation is based on the assumption that the detected power spectrum consists of superimposed, single-velocity Doppler histograms [Eq. (6)]. The validity of this assumption is strengthened by the results from the combined single and double-tube flow measurements (setup 4), as indicated in Fig. 4, where the additivity is shown.

A single-velocity component was estimated from the LDF data derived in experimental setup 1, using the observed flow velocity and a parabolic flow profile for simulating each reference spectrum. The result, displayed in Fig. 5, showed a close similarity between the VC and CMBC behavior. The results also displayed a slowly decreasing VC and CMBC with increasing velocities, even though a constant microsphere concentration was used.

The results from the single-tube flow measurements (setup 2) showed a linear relationship between VC and the microsphere concentration (Fig. 6). The velocity component was estimated using a single reference spectrum, based on the observed flow velocity 0.91 mm/s and a parabolic flow profile.
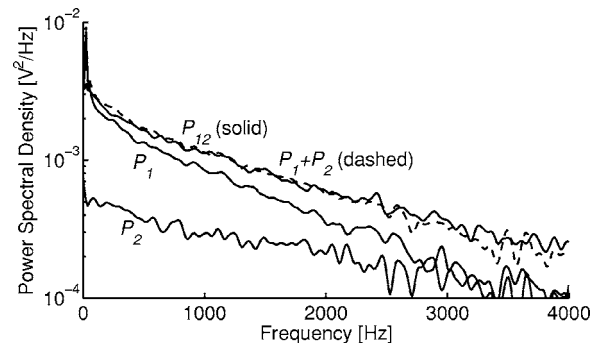


**Fig. 4** Example showing the additivity of Doppler spectra. The two single-flow spectra, measured at a velocity of 1.5 mm/s ($P_1$) and 7.7 mm/s ($P_2$), respectively (setup 4), add up to a spectrum ($P_1+P_2$) similar to a measured double-flow spectrum ($P_{12}$).
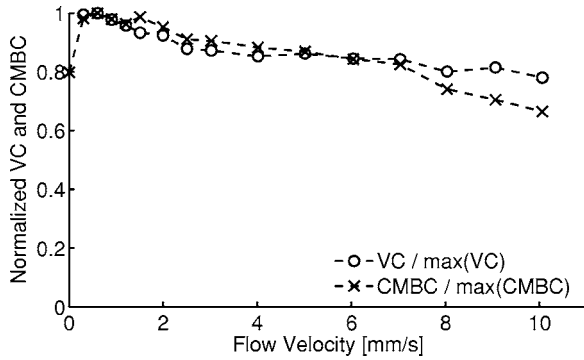
**Fig. 5** Estimations of CMBC and a single VC, derived from measurements at a single-tube flow of polystyrene microspheres with a velocity ranging from 0 to 10 mm/s (setup 1). Each VC was estimated using a single reference spectrum, based on the observed flow velocity and a parabolic flow profile.



**Fig. 7** Estimations of CMBC and three fixed VC ($c_{v_1}$, $c_{v_2}$, and $c_{v_3}$) derived from measurements at a single-tube flow of polystyrene microspheres with a velocity ranging from 0 to 10 mm/s (setup 1). The three reference spectra were simulated using a parabolic flow profile and the fixed velocities: $v_1 = 0.5$ mm/s, $v_2 = 2$ mm/s, and $v_3 = 8$ mm/s.

Previously presented VC results are calculated from spectra that were simulated using the observed flow velocity, an approach that is only applicable for model verification. In a real measurement setup, a few fixed velocity components must be selected. The results from VC estimations (setup 1), using reference spectra calculated from the three fixed velocities 0.5, 2, and 8 mm/s, are presented in Fig. 7. The three reference spectra were derived using a parabolic flow profile.

An example of the combined single and double-tube flow experiments (setup 3), using a polystyrene microsphere solution, is presented in Fig. 8. The displayed result was derived using simulated spectra that were fitted to the measured double-tube flow Doppler spectrum, i.e., no fitting against the single-tube flow measurements was conducted. Two reference spectra ($P_{v_1}$ and $P_{v_2}$) were simulated using the observed flow velocities $v_1 = 1.5$ (tube 1) and $v_2 = 7.7$ mm/s (tube 2), and a parabolic flow profile. Both the fitted spectrum and its two components ($P_{v_1}c_{v_1}$ and $P_{v_2}c_{v_2}$) showed a good agreement with the measured double- and single-tube flow spectra. The results from the other measurements that were conducted using setup 3 displayed a similar agreement when the relative difference between the velocities of the two tube flows was large.
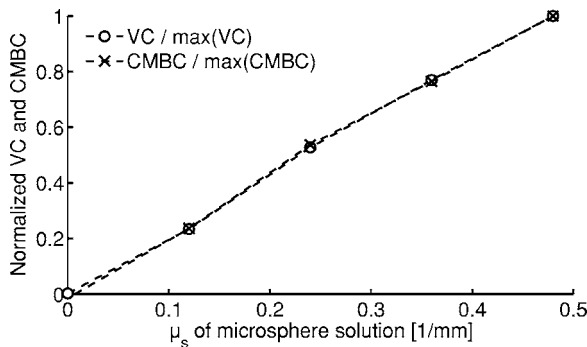
The results from the double-tube measurements, where a fixed microsphere concentration in tube 1 and an alternating microsphere concentration in tube 2 was used (setup 4), showed that it is possible to differentiate the two flows if the flow velocity differs between the tubes. The VC estimation algorithm, using the observed velocity of the two tubes (tube 1: 0.91 mm/s; tube 2: 2.90 mm/s) and a parabolic flow profile for simulating the two reference spectra, showed a linearly increasing concentration for the tube 2 component ($c_{v_2}$). No such increase was found in the tube 1 component ($c_{v_1}$), which displayed a constant behavior. The variations $[sd(c)/\bar{c}]$ in component $c_{v_1}$ ranged 11 to 23%. An example of the results is demonstrated in Fig. 9.

## 4 Discussion

In this paper, we proposed a method for separating different flow velocities in LDF. Typically, three concentrations, each associated with a predefined, physiologically relevant, absolute velocity (in millimeters per second), can be estimated simultaneously. The method is based on an analysis of the LDF Doppler spectrum, where a linear combination of predefined simulated single-flow spectra are fitted to a measured



**Fig. 6** Estimations of CMBC and a single VC derived from measurements at a single-tube flow of polystyrene microspheres with different concentrations (setup 2). VC reference spectra were simulated using the observed flow velocity 0.91 mm/s and a parabolic flow profile.
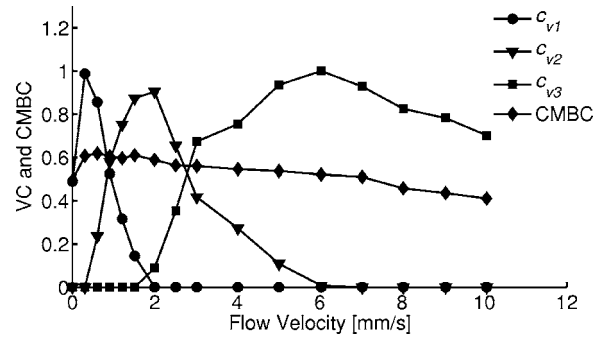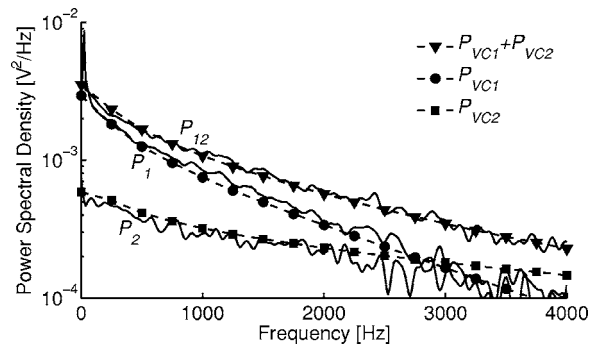


**Fig. 8** Decomposed measured double-tube flow spectrum (measured, $P_{12}$; component 1, $P_{VC_1} = c_{v_1}P_{v_1}$; component 2, $P_{VC_2} = c_{v_2}P_{v_2}$) as compared to measured single-tube flow spectra ($P_1$ and $P_2$), using setup 3. The reference spectra ($P_{v_1}$ and $P_{v_2}$) were simulated using the observed flow velocities $v_1 = 1.5$ and $v_2 = 7.7$ mm/s, and a parabolic flow profile. (solid: measured spectrum; dotted: simulated spectrum).
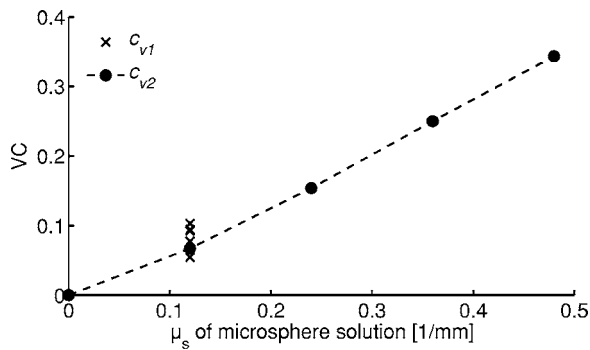
**Fig. 9** Two VC derived from a double-tube flow measurement series where the microsphere concentration in tube 1 was fixed ($\mu_s$ =0.12 mm⁻¹), while the microsphere concentration in tube 2 was altered (setup 4). The two velocity components ($c_{v_1}$ and $c_{v_2}$) were estimated using two reference spectra based on the observed flow velocities $v_1$=0.91 (tube 1) and $v_2$=2.90 mm/s (tube 2), and a parabolic flow profile.

spectrum. Numerous measurements were conducted on both single- and double-tube flow phantoms, using a polystyrene microsphere solution to validate the algorithm. The presented theory was also applied to RBC flow measurements to find an RBC phase function that produced simulation results that were consistent with the results from the measurements. The method was developed for low concentrations of scatterers (single Doppler scattering), but can theoretically be extended to the multiple Doppler scattering situation, as discussed in the following.

The simulation model includes an assumption of isotropic direction of the light. According to diffusion theory, this assumption is only valid if the photons have[17] traveled at least 1 mfp′. Based on the geometry of the flow phantoms, a reduced scattering coefficient of at least 0.4 mm⁻¹ is required, assuming negligible absorption. Preliminary oblique-angle measurements[18] indicate that the reduced scattering coefficient of the flow phantoms is about 1 mm⁻¹, i.e., the isotropic assumption holds. The simulation of the single-tube flow velocity spectrum also includes an assumption of a parabolic flow profile inside the tube. A maximal Reynolds number of 11 indicates that this assumption is valid. However, the fluid contains particles that might cause perturbations in the flow profile, even though the particle sizes are much smaller than the size of the tubes.

In the *in vivo* case, the RBCs tend to aggregate in the center of the microcirculatory vessels.[19,20] As a consequence, the RBC velocity distribution will be nonparabolic with an average RBC velocity greater than the flow velocity of the plasma. Therefore, in an *in vivo* setup, it is more appropriate to use a fixed velocity rather than the assumed parabolic profile. However, the resulting velocity components will not directly reflect the activity in either the capillaries or the arterioles, but rather the amount of RBC that flows with a specific velocity. Nevertheless, such a measure will contain valuable information about the microcirculation that cannot be found in the traditional integrated LDF perfusion measure.

The phase function of moving scatterers is difficult to characterize experimentally. Therefore, by using polystyrene microspheres, with a known radius and refractive index, we

were able to validate our model with an analytical phase function derived using Mie theory. The results showed a close match between the single-tube flow measurements and the simulations, with a few exceptions where a mismatch occurred in frequencies below 200 Hz. The origin of this mismatch is unclear to us, but possible explanations are disturbances in the laminar flow and/or air bubbles in the fluid. Nevertheless, our results indicate that the parabolic flow profile and isotropic assumptions are legitimate and that our model is valid in a low-concentration setup.

The results in this paper show that the Gegenbauer kernel phase function is suitable for modeling Doppler-scattering by red blood cells. By freely fitting the two Gegenbauer kernel parameters to measured LDF data, resulting in $\alpha_{gk}$=1.05 and $g_{gk}$=0.93 at 786 nm, we were able to achieve a good agreement between simulated and measured Doppler spectra. Comparing the LDF perfusion measure[5] (the first moment of the Doppler spectrum) generated by a Gegenbauer kernel phase function and a Heneye-Greenstein phase function with an identical anisotropy resulted in 3.6 times higher values for the Gegenbauer kernel phase function. This indicates the importance of using an accurate RBC phase function when simulating LDF perfusion and LDF Doppler spectra.

It was previously reported that Doppler shifts generated by moving polystyrene microspheres can be used for a precise estimation of the anisotropy factor.[16] Kienle et al. found an anisotropy factor of 0.993±0.001 at 820 nm for diluted blood by using the two-parameter Reynolds-McCormick phase function.[21] Others have reported that the two-parameter Gegenbauer kernel phase function is suitable for representing single scattering[12,13] by RBCs. Double sphere measurements, conducted by Roggan et al.,[12] showed that an $\alpha_{gk}$ of 1 yielded the closest match between measurements and theory. They found an anisotropy factor of $0.992 \leqslant g \leqslant 0.994$ at 633 nm for hematocrit values below 10. We found an $\alpha_{gk}$ of 1.05, which is in good agreement with their results. However, we found an anisotropy factor of 0.987 at 786 nm, which is lower than that of both Kienle and Roggan, but in good agreement with the anisotropy of 0.985 at 633 nm found by Steinke and Shepherd.[22] Some of these deviations are, of course, explained by the differences in wavelength. There are also methodologically induced errors due to the use of saline solution, which has a slightly different refractive index than blood plasma.[13] In addition, the phase function for whole blood, where the separations between red blood cells are small, is affected by interference between neighboring erythrocytes.[23] Hence, to find an appropriate phase function for modeling Doppler shifts by RBCs in real tissue, further studies are needed.

The proposed velocity component estimation method is capable of accurately estimating the relative concentration of moving scatterers in a single-tube flow phantom (Fig. 6). However, a slight dependency between the estimated concentration and the flow velocity was found (Fig. 5). The origin of this dependency is unclear, but a similar dependency was also found for the classical CMBC measure. Possibly, this might be explained by the extremely low degree of Doppler-shifted photons, a feature that results in an overall poor SNR. This ratio also decreases with increasing flow velocity. By increasing the concentration of moving scatterers, the degree of

Doppler-shifted photon can be raised. However, such an approach can cause unwanted nonlinear spectral effects due to multiple Doppler shifts and homodyne detection. The degree of Doppler-shifted photons[24] was estimated to be less than 0.4% in our setup.

Results from the double-tube flow measurements, using two velocity components, show that the LDF algorithm is capable of distinguishing two different tube flow velocities (Fig. 8) and to accurately estimate a microsphere concentration increase in one of the tubes (Fig. 9). Further, an estimate of at least three concentration measures, each reflecting the number of moving scatterers having a velocity close to a predefined flow velocity, can be achieved. This is demonstrated in Fig. 7, where the three velocity components 0.5, 2, and 8 mm/s are estimated from measurements on a single-tube flow model with alternating flow velocity. The true flow velocities, where the velocity component peak values are found, coincide well with their respective predefined velocities. In addition, the three peak values are almost equal in amplitude. Hence, the proposed LDF algorithm produces velocity-accurate concentration measures.

Our method was developed for low degrees of Doppler-shifted photons. For higher degrees of Doppler-shifted photons, nonlinearities are introduced due to homodyne mixing (shifted photons that are mixed with shifted photons) and multiple Doppler shifts. To make the velocity component algorithm valid in an *in vivo* measurement setup, where a high RBC concentration is expected, this limitation must be overcome. The homodyne mixing effect can be removed by deconvolution of the detected Doppler spectrum. A possible solution to the nonlinearities caused by the multiple Doppler shift is to adjust the simulated single-tube flow velocity spectra used in the fitting procedure. Serov et al.[24] previously presented a way of estimating the degree of Doppler-shifted photons. By combining their results with a Poisson distribution assumption regarding the distribution of multiple Doppler shifts, simulations of multiple Doppler-shifted reference spectra might be achieved.

The classical LDF perfusion measure claims to estimate the RBC concentration times the RBC average velocity. It is a nonabsolute measure that often is calibrated against a motility standard solution consisting of polystyrene microspheres diluted in water. Thus, the perfusion measure is related to the phase function of a microsphere rather than an RBC. The polystyrene microspheres used in this paper resulted in an almost 15 times higher LDF perfusion estimate compared to the RBCs at a similar velocity. Instead, our approach takes into account the phase function of the RBC, which potentially enables the measurement of absolute RBC velocities. However, it is still a nonabsolute measure when it comes to estimating the concentration of moving scatterers at a certain velocity. To achieve an absolute RBC concentration measure, the photon path length in tissue is required.[5,25] Nilsson et al.[26] and Larsson et al.[27] showed that it is possible to estimate the photon path length by studying the spatially resolved diffuse reflectance profile, using a multichannel LDF probe. Hence, in theory, it is possible to measure microcirculatory velocities and concentrations in absolute units using LDF, by combining these techniques. However, in real tissue, where the blood flow is localized to the microcirculatory blood vessels, the applicability can be questioned. The robustness of the pro-

posed LDF algorithm must be evaluated further in a tissue-like heterogeneous model, as can be achieved through Monte Carlo simulations.

An attempt to create a velocity-resolved perfusion measure was previously conducted by Dörschel and Müller.[6] Their approach was based on the differential quotient of the LDF Doppler spectrum to correct for the isotropic nature of the scattering vector. Hence, they only partially solved the problem, as they did not account for the phase function of the moving scatterers. Their approach can be questioned since it is only theoretically valid for a fixed relation between the scattering vector and the direction of the moving scatterer. Yet, they present convincing results from phantom measurements, using a piece of static scattering thin Teflon® foil placed above a moving piece of paper. The dimension and optical properties of their Teflon® foil is, however, not specified, and thus, it cannot be excluded that their results originate from a non-physiologically relevant phantom setup, where the scattering vector and the direction of the moving scatterer has a fixed nonisotropic relationship.

Several authors previously suggested algorithms that estimate the blood flow root mean square (rms) velocity $v_{rms} = \langle v_{RBC}^2 \rangle^{1/2}$ in absolute terms. Lohwasser and Soelker[7] matched measured Doppler spectra with Monte Carlo simulations and diffusing wave spectroscopy results. They found that by using a large emitting-receiving fiber separation (25 to 60 mm) it was possible to estimate $v_{rms}$. However, they did not consider that the Doppler spectrum depends on the optical properties ($\mu_a$ and $\mu_s'$) of the turbid medium, as shown by Kienle.[8] Kienle proposes that by matching simulated spectra, derived using the correlation diffusion equation, with measured spectra, and simultaneously determining the optical properties, an accurate $v_{rms}$ estimate can be achieved. This approach is, however, valid only for large emitting-receiving fiber separations, i.e., a high degree of multiple Doppler shifts, where the Doppler spectrum only depends on $\mu_s'$ and not the anisotropy.[8,28] Binzoni et al.[9] suggested an alternative approach that takes multiple Doppler shifts into account. Their approach, based on a theoretical framework by Bonner and Nossal[3] assumes a Gaussian RBC velocity distribution in the tissue and that the RBC phase function is described by the Rayleigh-Gans approximation. However, the Rayleigh-Gans approximation is accurate only in describing RBC scattering in the 0- to 4-deg range,[13] and thus, this approach might not be suitable for small source detector separations (low degrees of multiple Doppler shifts) where the phase function has a profound influence on the Doppler spectrum. It has also been shown that $v_{rms}$ is estimated by the ratio between the first moment of the Doppler spectrum and the zeroth moment.[29] However, this is valid only if the degree of multiple Doppler shifts is negligible, since the zeroth-moment concentration estimate rapidly becomes nonlinear if multiple Doppler shifts are present. By applying a linearization algorithm[4,24] to the LDF concentration measure, it might be possible to use the technique in LDF probe setups similar to ours. Still, this approach is capable of estimating only the average RBC velocity, and not multiple velocity components.

What are the possible clinical implications of measuring microcirculatory blood flow in absolute units? Clinicians are used to measuring blood flow in larger vessels in absolute

units. By measuring the microcirculatory flow velocity in absolute units, a better acceptance and integration of the method with other blood flow measuring methods can be assumed. In addition, the proposed algorithm might be used for monitoring the tissue perfusion associated with a specific blood flow velocity interval. As the blood flow velocity depends on the dimension of the blood vessel, it might be possible to differentiate between microcirculatory compartments. If successful, this would enable the estimation of the true nutritive capillary blood flow and the detection of shunted blood flow, as associated with diseases and conditions affecting the microcirculation, such as diabetes and leg ulcers.

## 5   Conclusions

We proposed an LDF algorithm for velocity-resolved perfusion measurements. The proposed method yields three concentration measures, each associated with a predefined, physiologically relevant, absolute velocity in millimeters per second. Validation measurements, using both single- and double-tube flow phantoms and a microsphere solution, showed that it is possible to track velocity and concentration changes, and to differentiate between flows with different velocities. *In vivo*, this might enable the differentiation between capillary and arterial blood flow, as the velocity depends on the dimension of the blood vessel. However, further studies are needed to validate the applicability in real tissue. The presented theory was also applied to RBC *in vitro* flow measurements. A Gegenbauer kernel phase function ($\alpha_{gk} = 1.05$; $g_{gk} = 0.93$), with an anisotropy factor of 0.987 at 786 nm, was found suitable for modeling Doppler scattering by RBCs diluted in saline solution. The method was developed for low concentrations of RBCs, but can in theory be extended to cover multiple Doppler scattering. The current LDF algorithm yields only concentration measures that are relative, but by adding a path length estimation technique, a velocity-resolved absolute LDF perfusion measure might be achievable.

### References

1. H. Z. Cummins and H. L. Swinney, "Light beating spectroscopy," in *Progress in Optics*, Vol. VIII, pp. 135–200, North Holland Publishing Co., Amsterdam (1970).
2. G. E. Nilsson, T. Tenland, and P. Å. Öberg, "Evaluation of a laser Doppler flowmeter for measurement of tissue blood flow," *IEEE Trans. Biomed. Eng.* **27**(10), 597–604 (1980).
3. R. F. Bonner and R. Nossal, "Model for laser Doppler measurements of blood flow in tissue," *Appl. Opt.* **20**(12), 2097–2107 (1981).
4. G. E. Nilsson, "Signal processor for laser Doppler tissue flowmeters," *Med. Biol. Eng. Comput.* **22**(4), 343–348 (1984).
5. R. F. Bonner and R. Nossal, "Principles of laser-Doppler flowmetry," in *Laser-Doppler Blood Flowmetry*, A. P. Shepherd and P. Å. Öberg, Eds., pp. 17–45, Kluwer Academic, Boston (1990).
6. K. Dörschel and G. Müller, "Velocity resolved laser Doppler blood flow measurements in skin," *Flow Meas. Instrum.* **7**(3–4), 257–264 (1996).
7. R. Lohwasser and G. Soelkner, "Experimental and theoretical laser Doppler frequency spectra of a tissuelike model of a human head with capillaries," *Appl. Opt.* **38**(10), 2128–2137 (1999).
8. A. Kienle, "Non-invasive determination of muscle blood flow in the extremities from laser Doppler spectra," *Phys. Med. Biol.* **46**(4), 1231–1244 (2001).
9. T. Binzoni, T. S. Leung, D. Boggett, and D. Delpy, "Non-invasive laser Doppler perfusion measurements of large tissue volumes and human skeletal muscle blood rms velocity," *Phys. Med. Biol.* **48**(15), 2527–2549 (2003).
10. G. E. Nilsson, E. G. Salerud, T. Strömberg, and K. Wårdell, "Laser Doppler perfusion monitoring and imaging," in *Biomedical Photonics Handbook*, T. Vo-Dinh, Ed., CRC Press LLC, Boca Raton, FL (2003).
11. A. T. Forrester, "Photoelectric mixing as a spectroscopic tool," *J. Opt. Soc. Am.* **51**(3), 253–259 (1961).
12. A. Roggan, M. Friebel, K. Dorschel, A. Hahn, and G. Muller, "Optical properties of circulating human blood in the wavelength range 400–2500 nm," *J. Biomed. Opt.* **4**(1), 36–46 (1999).
13. M. Hammer, D. Schweitzer, B. Michel, E. Thamm, and A. Kolb, "Single scattering by red blood cells," *Appl. Opt.* **37**(31), 7410–7418 (1998).
14. C. F. Bohren and D. R. Huffman, *Absorption and Scattering of Light by Small Particles*, Wiley-Interscience, New York (1983).
15. F. Kreith and S. A. Berger, "Fluid mechanics," in *Mechanical Engineering Handbook*, F. Kreith, Ed., CRC Press LLC, Boca Raton, FL (1999).
16. A. Kienle, M. S. Patterson, L. Ott, and R. Steiner, "Determination of the scattering coefficient and the anisotropy factor from laser Doppler spectra of liquids including blood," *Appl. Opt.* **35**(19), 3404–3412 (1996).
17. J. Mobley and T. Vo-Dinh, "Optical properties of tissue," in *Biomedical Photonics Handbook*, T. Vo-Dinh, Ed., CRC Press LLC, Boca Raton, FL (2003).
18. L. H. Wang and S. L. Jacques, "Use of a laser-beam with an oblique angle of incidence to measure the reduced scattering coefficient of a turbid medium," *Appl. Opt.* **34**(13), 2362–2366 (1995).
19. T. W. Secomb, "Mechanics of red blood cells and blood flow in narrow tubes," Chap. 4 in *Modeling and Simulation of Capsules and Biological Cells*, C. Pozrikidis, Ed., pp. 163–190, Chapman & Hall/CRC Mathematical Biology and Medicine Series, Boca Raton, FL (2003).
20. A. S. Popel and R. N. Pittman, "Mechanics and transport in the microcirculation," Chap. 31 in *The Biomedical Engineering Handbook*, 2nd ed., J. D. Bronzino, Ed., CRC Press LLC, Boca Raton, FL (2000).
21. L. O. Reynolds and N. J. McCormick, "Approximate two-parameter phase function for light scattering," *J. Opt. Soc. Am.* **70**(10), 1206–1212 (1980).
22. J. M. Steinke and A. P. Shepherd, "Comparison of Mie theory and the light-scattering of red blood-cells," *Appl. Opt.* **27**(19), 4027–4033 (1988).
23. M. Hammer, A. N. Yaroslavsky, and D. Schweitzer, "A scattering phase function for blood with physiological haematocrit," *Phys. Med. Biol.* **46**(3), N65–N69 (2001).
24. A. Serov, W. Steenbergen, and F. F. M. de Mul, "Prediction of the photodetector signal generated by Doppler-induced speckle fluctuations: theory and some validations," *J. Opt. Soc. Am. A* **18**(3), 622–630 (2001).
25. R. Nossal, R. F. Bonner, and G. H. Weiss, "Influence of path-length on remote optical sensing of properties of biological tissue," *Appl. Opt.* **28**(12), 2238–2244 (1989).
26. H. Nilsson, M. Larsson, G. E. Nilsson, and T. Strömberg, "Photon pathlength determination based on spatially resolved diffuse reflectance," *J. Biomed. Opt.* **7**(3), 478–485 (2002).
27. M. Larsson, H. Nilsson, and T. Strömberg, "In vivo determination of local skin optical properties and photon path length by use of spatially resolved diffuse reflectance with applications in laser Doppler flowmetry," *Appl. Opt.* **42**(1), 124–134 (2003).
28. G. Soelkner, G. Mitic, and R. Lohwasser, "Monte Carlo simulations and laser Doppler flow measurements with high penetration depth in biological tissuelike head phantoms," *Appl. Opt.* **36**(22), 5647–5654 (1997).
29. A. P. Shepherd and P. Å. Öberg, *Laser-Doppler Blood Flowmetry*, Vol. 107 of Developments in Cardiovascular Medicine, Kluwer Academic, Boston (1990).